

Material removal behavior in scratching of zirconia ceramic surface treated with laser thermal shock

Sheng Xu^{1,3} · Zhenqiang Yao^{1,2,3} · Manchao Zhang¹

Received: 4 June 2015 / Accepted: 11 November 2015 / Published online: 23 November 2015
© Springer-Verlag London 2015

Abstract Laser thermal shock (LTS)-assisted grinding is a novel technology for processing ceramics. However, the material removal mechanism in LTS-assisted grinding has not been studied extensively, hindering the sufficient development of its potential. This paper focuses on the material removal mechanism in LTS-assisted grinding by investigating the material removal behavior in LTS-assisted scratching of yttria-stabilized tetragonal zirconia polycrystal (Y-TZP). In order to reveal the different material removal behaviors between the Y-TZP specimen surfaces with and without LTS, the scratch characteristics were investigated and compared in terms of hardness of the ceramic surface, scratching force ratio (SFR), and scratch morphology. Compared with the surface without LTS, the grooves on the surface with LTS were deeper, the SFR was larger, and the hardness of surface decreased. These results indicate that the grindability of Y-TZP significantly improved from the assistance of the LTS. As further evidence, prominent marks of grain spalling were found in the scratch grooves on the surface with LTS and the material removal volume increased. These results indicate that the cutting efficiency of the tool improved after the

surface was treated with LTS. Furthermore, the plastic ridges and marks of grain spalling on the surface assisted with LTS indicate the existence of ductile-brittle mixed mode. This is significant and beneficial for ceramics grinding due to its improved surface integrity and large material removal rate.

Keywords Laser thermal shock-assisted scratching · Material removal mechanism · Y-TZP · Hardness · Scratch characteristics

1 Introduction

Advanced ceramic materials are used due to their unique combination of physical and mechanical properties, which include high hardness, good wear resistance, chemical inertness, and low density. These features have led to the wide use of advanced ceramics materials in applications for the nuclear industry, aerospace industry, and automotive components, and with biocompatible implants [1–4]. However, the same properties that make ceramics attractive for these applications also create challenges with their machining. Machining is unavoidable due to the high dimensional accuracy and surface integrity required in the above industries [3, 5–7]. Ceramics grinding is currently the preferred method to perform this machining [8, 9]. However, low machining efficiency and rapid grinding wheel consumption are major concerns with the current approach. Better understanding of the material removal mechanisms is a logical and necessary step to make improvements in these regard. The grinding process is the result of individual abrasive grains engaging in cutting actions. Thus, the investigations into material removal mechanisms of grinding are primarily based on abrasive scratch tests. Therefore, in order to improve the potential of ceramics grinding based on

✉ Sheng Xu
story2011@sjtu.edu.cn

✉ Zhenqiang Yao
zqyaosjtu@gmail.com

¹ State Key Laboratory of Mechanical System and Vibration, Shanghai 200240, People's Republic of China

² Gas Turbine Research Institute, Shanghai Jiao Tong University, Shanghai 200240, People's Republic of China

³ School of Mechanical Engineering, Shanghai Jiao Tong University, Minhang District, 200240 Shanghai, People's Republic of China

material removal mechanisms, the abrasive scratch process was the initial area of study [5, 7, 10–15].

Sivakumar [10] investigated the different wear behaviors based on scratch tests conducted by a smooth and rough stylus. The results indicated that the scratch process with a rough stylus was comparable to severe wear, which includes the increased probability of crack formation. According to the viewpoint of Desa [7], who concluded that grinding is an accelerated abrasive wear process, severe wear is essentially an efficient form of material removal, which is desired in ceramics grinding. The results of scratch tests suggested that the use of rough abrasive could achieve large material removal rates. For surface/subsurface damage, Kanematsu [11] conducted scratch tests with progressive loads in order to determine the relationship between damage characteristics and mechanical response of materials. Based on results of these tests, factors concerning the relative merits of each zirconia type such as wear properties, contact fatigue, and machining damage were briefly discussed [12]. Noting that most scratch tests were conducted in dry conditions, Desa [7] conducted single point, unidirectional scratch tests in different lubricant conditions to examine how the lubricants affected subsurface damage and material removal in the scratch process. Subhash [13] developed a new model to reflect the susceptibility of a ceramic to scratching-induced damage. The findings above for material removal behavior in scratch tests serve as the basis for pursuing further improvements in ceramic grinding.

This progress notwithstanding, the above research has been limited to conventional scratching, which uses an entirely mechanical process. In recent years, hybrid manufacturing technologies such as ultrasonic vibration-assisted machining, laser-assisted machining, and electrical discharge grinding [5, 16–19] have attracted much attention due to expected improvements in machining time, costs, quality, or precision. To research and develop hybrid manufacturing techniques, hybrid scratch tests have been conducted. Feng [5] investigated the difference between ultrasonic vibration-assisted and conventional scratching to reveal the mechanism of ultrasonic vibration-assisted process. He confirmed that ultrasonic vibration-assisted scratch contributed to additional material removal. Rebro [16] studied the laser-assisted machining of mullite. This technique weakened the work material through thermal softening and then the softened material was removed immediately. They successfully performed crack-free laser-assisted machining of mullite. However, this technology currently needs reforming equipment. The expense of this equipment is an obstacle to the adoption of the technology.

More recently, Kumar [4] and Zhang [9, 20] developed a novel two-step hybrid process to grind ceramics. First, the ceramic was irradiated by laser. During laser irradiation, the rapid heating and cooling process, called laser thermal shock (LTS), caused steep temperature gradients. These gradients weakened the strength of the material surface [4]. Following

this step, the weakened material was removed by grinding. This process was very different from the technique of weakening the work material through thermal softening. This process was proved to be feasible for ceramic micro-grinding and macro-grinding [4, 9, 20]. However, investigation into the material removal mechanism of the process has not been conducted.

The current research was conducted to determine the material removal behavior of Y-TZP ceramic surfaces treated with LTS. This can provide a basis for understanding the material removal mechanism. Single-point scratch tests were used in current study in order to avoid the interaction between cracks originating from surrounding contacts. The SFR, scratch morphology, and material removal volume were investigated and compared for Y-TZP ceramics surfaces with and without LTS.

2 Experimental conditions and procedures

2.1 Materials

Y-TZP (supplied by Shanghai Institute of Ceramics, Chinese Academy of Sciences) served as the object ceramic material due to its susceptibility to thermal shock. The testing surface of each specimen was grinded and then polished sequentially with 15, 6, 3, and 1 μm diamond paste. The surface roughness was then measured by a 3D profilometer. The mean value of roughness (R_a) was 16 nm. For scratch testing, the ceramic specimen was cut into pieces with dimensions of 15 (L) mm \times 10 (W) mm \times 5 (D) mm. The relevant mechanical and thermal properties are given in Table 1.

2.2 Setup and conditions

Prior to LTS, a layer of carbon powder was sprayed on the polished surface in order to change the surface from specular to diffuse.

An IPG fiber laser (CW) was employed to irradiate the ceramic surface. The laser power used in the experiments was 187 W. The scan speed was 60 mm/min. The spot diameter was approximately 2 mm. To avoid the interaction of two laser tracks, 3 mm was adopted as the distance between two laser tracks based on the results of pre-experiments. Figure 1a shows the experimental apparatus for laser irradiation, and Fig. 1b shows the laser irradiation tracks.

The temperature of the ceramic surface during the experiment was monitored by an infrared imaging system (SC7700, FLIR Systems Inc., USA). According to the records, the temperature of specimen increased from room temperature during laser spot moving along each track. Some of the temperature results are shown in Fig. 2. The maximum temperature was 645 $^{\circ}\text{C}$ which is below the melting point of Y-TZP (2716 $^{\circ}\text{C}$)

Table 1 The relevant mechanical and thermal properties

Material	Elasticity modulus/ GPa	Poissons ratio	Yield stress/ MPa	Density g/mm ³	Specific heat capacity J/Kg°C	Conductivity W/mm°C
Y-TZP	210	0.3	1240	6.02	450	2.0×10^{-3}

[21]. Therefore, no recasting layer existed on the specimen surface after laser irradiation. Figure 2b illustrates that the ceramic surface experienced large temperature gradients. This large temperature gradient modified the surface integrity according to the characteristics of Y-TZP. These changes can be a benefit to ceramics grinding due to the “size effect” that more defects per unit volume result in better grindability [22, 23].

Note that the temperature gradient before the laser spot was larger than the temperature gradient after the laser spot (Fig. 2b). The volume of the localized region under laser spot expanded due to heating from the laser spot. Based on these observations, it can be concluded that the part of specimen located before the laser spot experienced the most tensile stress. The large temperature gradient in this region also increased the likelihood of defects.

After laser irradiation, the ceramic specimen was cleaned with an ultrasonic washer in acetone for 5 min. The hardness tests were then conducted by Microhardness Tester (Shanghai Taiming Optical Instrument Co., Ltd, China). Utilizing an optical microscope, the indentations morphologies were recorded.

Scratch tests were performed using a lateral force measurement technology attached to a Nano Indenter XP (Agilent Technologies, Inc., USA). A Berkovich indenter was also employed. Every scratch test was done at the center of laser tracks, as shown in Fig. 3. All the scratches were in the same direction and parallel to the laser tracks. Every scratch test was conducted according to a three-step procedure [14, 24]. First, a pre-scan was performed at a very small load (20 μ N) to obtain

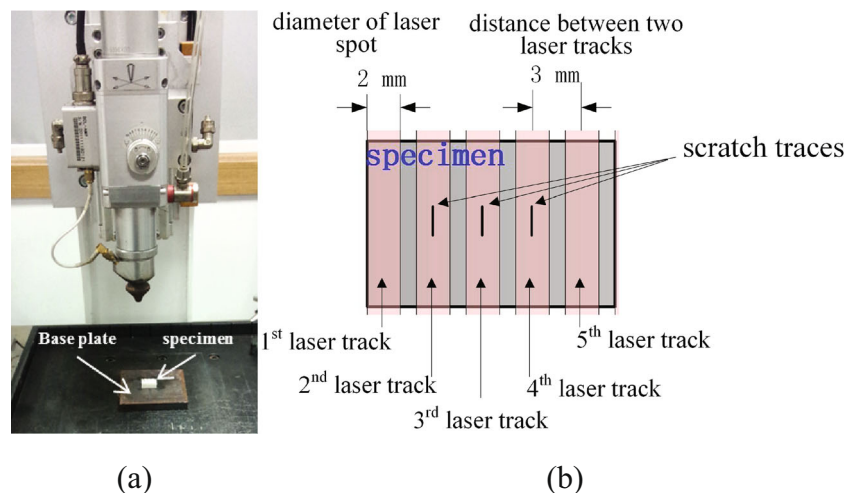
the initial specimen surface profile. Second, the “true” scratch test was conducted. A progressive load from 0 to 200 mN was applied. The length for each scratch was 2500 μ m. The scratch speed was 10 μ m/s. During scratching, the scratch depths and applied load were recorded. Finally, the surface profile of the specimen was scanned again with the identical procedure as in the pre-scanning. The distance between two scratches was large enough to avoid any interaction [14]. Control experiments were conducted by repeating all procedures on a ceramic surface not treated with LTS. The air temperature was 25 °C, and the relative humidity was 40–50 % throughout the experiment.

The 3D shapes of scratch grooves on the surface with and without LTS were recorded by True Color Confocal Microscope (Axio CSM 700, Carl Zeiss Co. Ltd., Germany). Scratch morphology and material removal volume were obtained based on the 3D shapes.

3 Results and discussion

Single-point scratching can avoid the interaction of abrasions, temperature, and coolant liquid during the grinding process. Understanding the material removal behavior in scratching of ceramics is essential for thoroughly analyzing the material removal mechanism during the grinding process. Based on single-point scratch tests, this current study aimed to reveal the difference of material removal mechanism between a surface treated with and without LTS.

Fig. 1 a Schematic of irradiation experimental setup; b the laser irradiation track



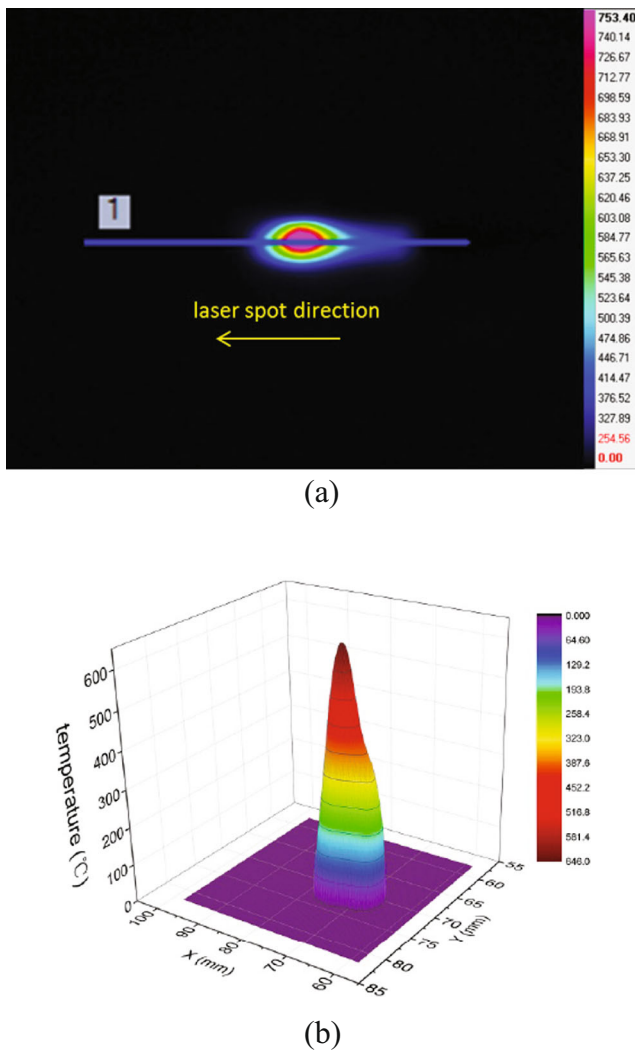


Fig. 2 Temperature field on the specimen surface during laser irradiation: **a** image captured by infrared imaging system; **b** temperature distribution

3.1 Hardness and the depth of the weakened layer

In order to check the weakened layer introduced by LTS, the specimen was cut into two pieces and the cross-section (face

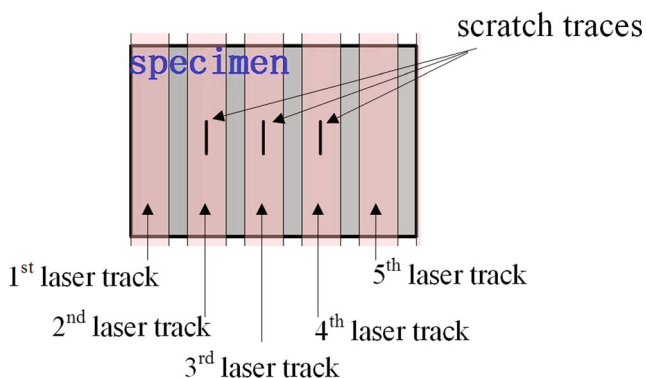


Fig. 3 The laser tracks and the scratch traces

1) was polished. The cross-section micrographs of the weakened layer were obtained by True Color Confocal Microscope (Fig. 4). It can be drawn that the weakened layer did not separated from the base material, as shown in Fig. 5.

Hardness is an important material property which has a great effect on manufacturing of materials. The hardness of the ceramic surface with and without LTS was different. The average value of hardness on the surface with LTS was 1143HV while the value of surface without LTS was 1258HV, which represents a significant decrease of 9 % after the specimen was treated with LTS. Furthermore, the hardness of the specimen with LTS increases with the increasing of the depth, as shown in Fig. 6. The procedure to obtain the relationship between the hardness and the depth is shown in Fig. 7. When the weakened layer was removed completely, the hardness of the material would be stable. Based on Fig. 6, the thickness of the weakened layer is about 188 μm .

This reduction in hardness represents a weakening of the surface material strength. It also means that the normal grinding force can decrease [25]. The reduction of normal grinding force is benefit to the increase of the grinding wheel life.

A radial microcrack was observed on the surface treated with LTS, as shown in Fig. 8b. The indentations with long microcracks were always located in the laser irradiation tracks. Not all of indentations on the surface were with long microcracks. The other microcracks attaching to these indentations which located near the middle part between neighboring laser irradiation tracks were short.

3.2 Scratch groove morphology

Scratch groove morphology is a visual result of the material removal mechanism. The ridges and cracks symbolize ductile mode and brittle mode, respectively. The 3D shapes of typical scratch grooves on the surface treated with and without LTS were recorded by a True Color Confocal Microscope, as shown in Fig. 9. The white regions beside the grooves in Fig. 9a, b were the ridges formed by plastic deformation. It should be noted that the white regions in Fig. 9a were more obvious than those in Fig. 9b. It is concluded that the plasticity of the surface without LTS is larger than the surface with LTS. This is beneficial to minimize the microcracks caused by

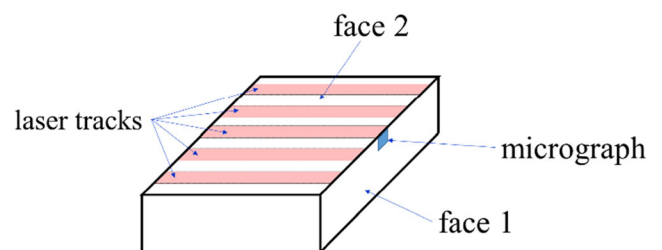


Fig. 4 Schematic of the sample to study the weakened layer

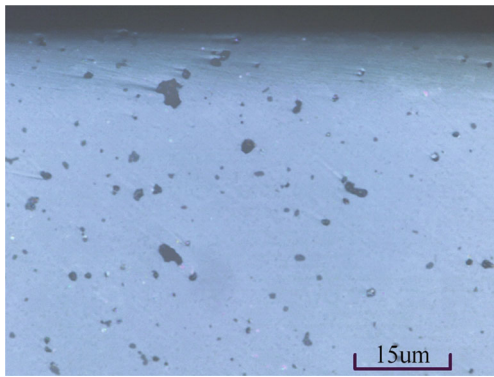


Fig. 5 The micrograph of the cross-section of the weakened layer

grinding but correspondingly is not beneficial for removing material.

The outlines of the cross-section perpendicular to the scratch direction are shown in Fig. 9a, b. The locations of cross-section are indicated by the yellow lines. The depth and width of grooves were measured based on the images. Because the bottoms of the grooves were not even, a novel approach to measure the depth was necessary. Measurement locations along the centers of the grooves were determined and are marked by yellow lines in Fig. 9c, d. Figure 9c shows that the actual scratch depth on the surface not treated with LTS was approximately 320 nm while the depth of surface treated with LTS was 437 nm, as shown in Fig. 9d. The location of the measurement ranged from 2105 to 2160 µm in which the normal load was constant, as shown in Fig. 10. The depth of grooves on the LTS-treated surface was therefore 37 % larger than the polished surface. These results indicate that LTS will make a ceramic surface easier to penetrate in the grinding process. The possibility of grinding with a lower normal grinding force is significant because a large normal grinding force is more likely to damage the finish surface [26].

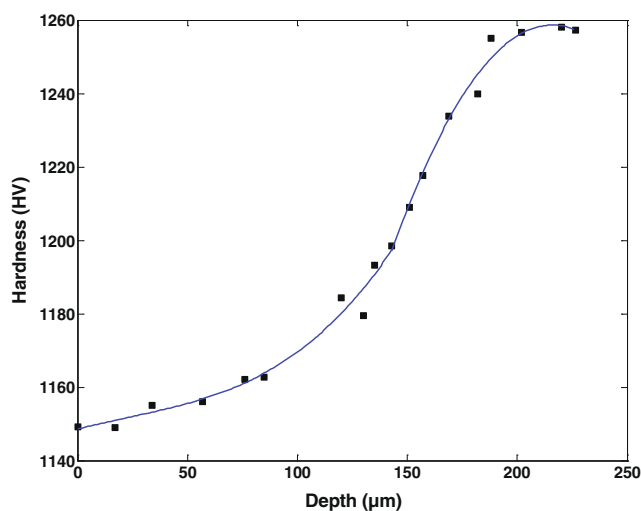


Fig. 6 The hardness versus the depth

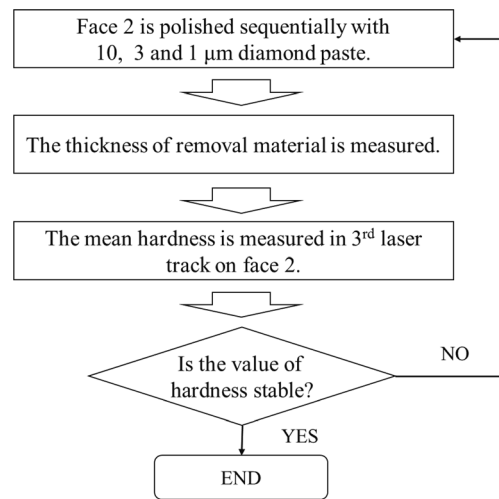


Fig. 7 The procedure to obtain the hardness in different depth

It is should be further noted that the grooves on the surface not treated with LTS were more smooth while many marks of grain spalling were found on the surface treated with LTS. No microcracks were found on these two surfaces, which indicate that the microcracks around the indentation described in Section 3.1 may contribute to grain spalling in the scratch process. Grain spalling can decrease the possibility of crushing to large particles. It is an expected phenomenon in ceramics grinding due to the larger material removal rate than a ductile mode and a better surface integrity than a brittle mode. It is therefore expected that the process of LTS may not cause deteriorating surface integrity during grinding. The appearance of grain

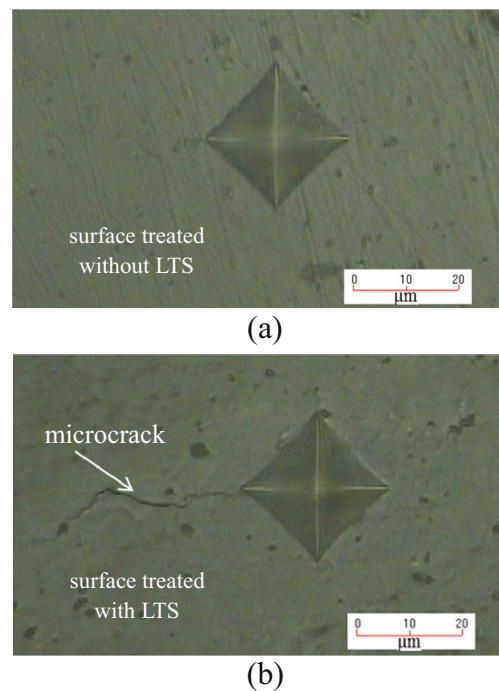


Fig. 8 a Indentation on the surface treated without LTS, b indentation on the surface treated with LTS

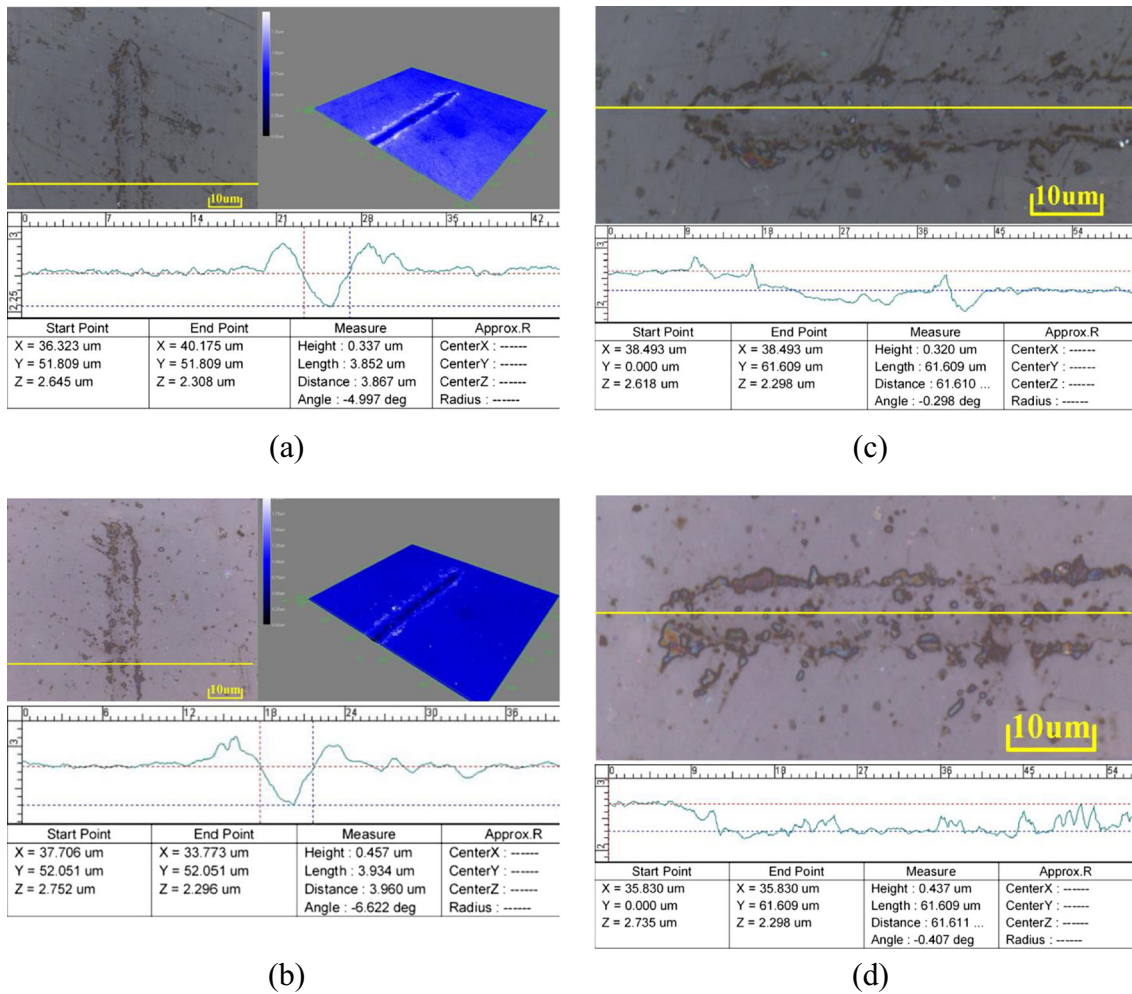


Fig. 9 Scratch groove morphology and the cross section outlines of scratch grooves. The locations of the cross-section outlines were at the yellow lines. **a** Cross-section of scratch groove on surface treated without

LTS; **b** cross-section of scratch groove on surface treated with LTS; **c** the depth of the scratch groove on surface treated without LTS; **d** the depth of the scratch groove on surface treated with LTS

spalling and ridges indicates that the material removal mechanism changes from ductile mode to ductile-brittle mixed mode.

3.3 Scratching force ratio

Scratching force ratio (SFR) is an important parameter in ceramics grinding because it describes the grindability of ceramics. The SFR for each scratch test was obtained from the equation $SFR = Ft/Fn$, where Ft is the tangential load and Fn is the normal load. In the scratch process, Ft has a dominant effect on material removal rate, and Fn determines the abrasive penetration into the material. Previous studies have shown that the SFR of scratching can reveal the properties of material removal [5, 27]. The SFR mainly depends on the grindability of workpiece material [28]. The larger the SFR becomes, the higher the grindability of workpiece material is [29].

In the current tests, the normal load was gradually increased from 0 to 200 mN, as shown in Fig. 10. Because

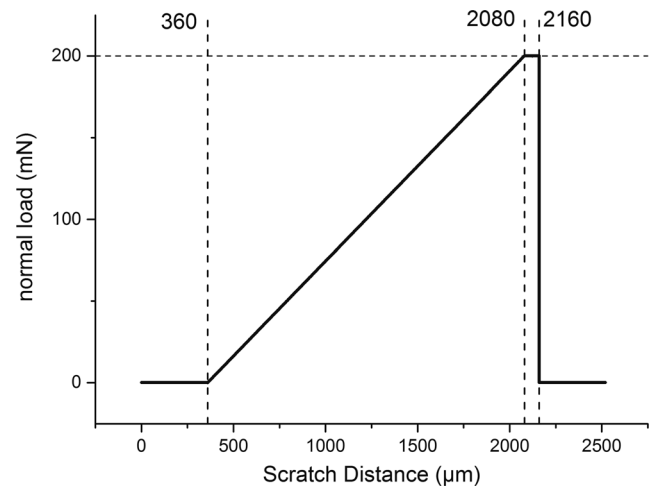


Fig. 10 Normal load applied along the scratch track

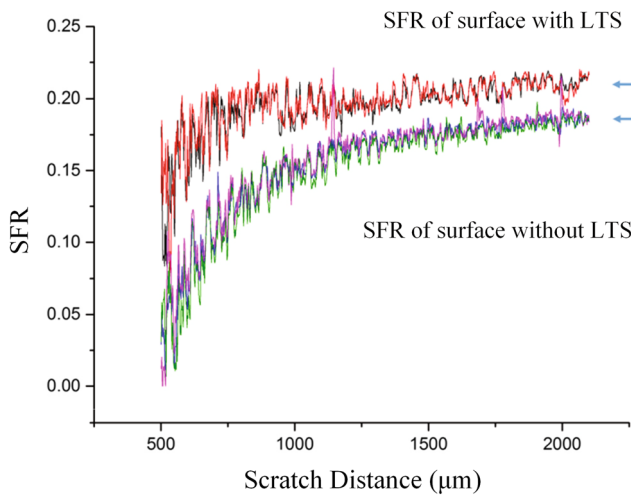


Fig. 11 Comparison of the SFR of surfaces with and without LTS

the loads at the beginning and the end of the scratches were zero, only the middle part of each scratch process was analyzed.

To obtain the SFR measurements, scratch tests were first conducted on the surfaces treated with LTS. The tests were then repeated on the surface without LTS. All of the results are shown in Fig. 11. The SFR was small at the beginning of each scratch and then gradually increased as the normal load increased. The SFR increased slightly when the normal force exceeded 100 mN. The asymptotic values of SFR for the

surface with and without LTS were approximately 0.21 and 0.18, respectively. The dramatic effects of treating the surface with LTS are apparent with a SFR increase of 16.7 %.

This increase of SFR is exciting because Ft ($Ft = SFR \times Fn$) will increase when SFR increases for a given Fn . Ft has a significant effect on material removal. Therefore, the larger SFR will produce larger material removal volume, which is a benefit to ceramics grinding. The conclusion is confirmed in Section 3.4 of this paper. Likewise, for conditions with identical material removal, a larger SFR corresponds to a smaller Fn , which can produce less surface/subsurface damage [26] and longer grinding wheel life. A smaller Fn also minimizes radial and median crack propagation [30], which should help maintain surface integrity.

3.4 Material removal volume

The results above have demonstrated that LTS on a ceramic surface can reduce the normal machining force for ceramic grinding. In order to determine whether the LTS on a ceramic surface can also enhance the material removal rate, the volume of ridges and grooves was measured. The typical results are shown in Fig. 12. The volume was measured at the end of the grooves where 200 mN was applied. The lengths of the measured areas were approximately 55 μm.

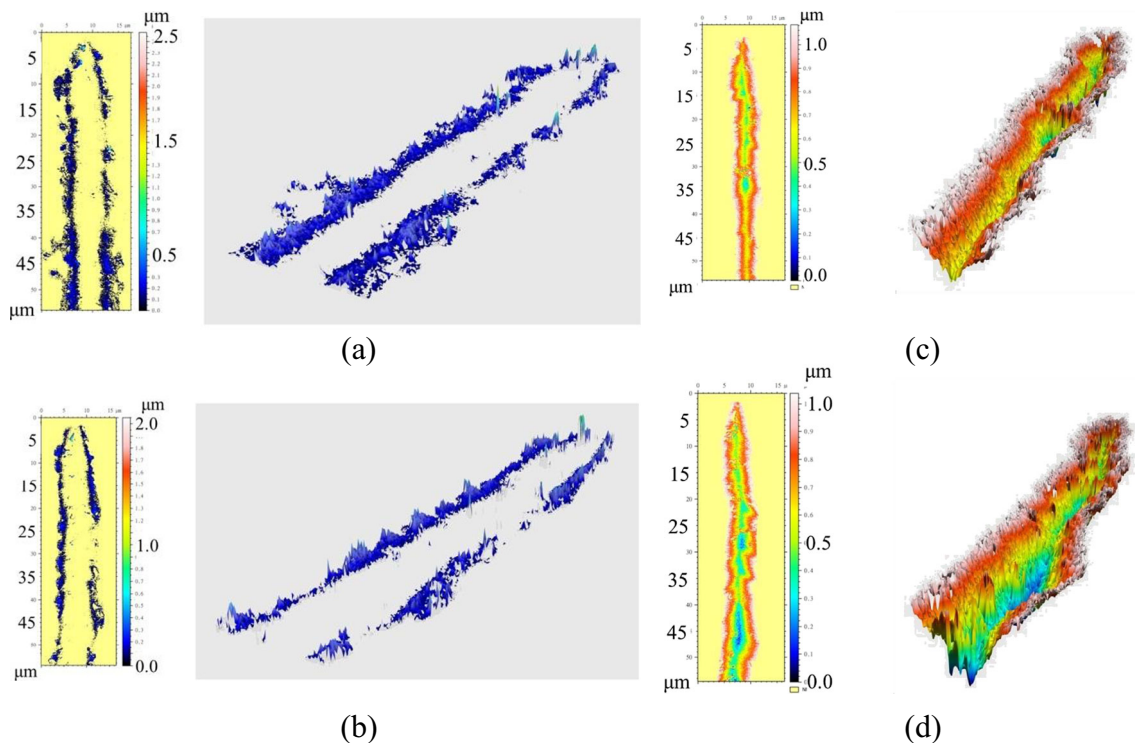


Fig. 12 3D graphics of scratch marks: **a** ridges on the surface treated without LTS; **b** ridges on the surface treated with LTS; **c** groove on the surface treated without LTS; **d** groove on the surface treated with LTS

In Fig. 12a, the ridges caused by plastic deformation were conspicuous on the surface not treated with LTS. The volume of these ridges was approximately $16.5 \mu\text{m}^3$. The volume of the groove in Fig. 12c was approximately $67.3 \mu\text{m}^3$. Thus, the material removal volume of the scratch on the surface without LTS was $50.8 \mu\text{m}^3$. In Fig. 12b, the ridges on the surface with LTS were not conspicuous because the micro-chips formed by scratching were cleaned with an ultrasonic washer for 5 min. The volume of these ridges was $10.3 \mu\text{m}^3$. The volume of the groove in Fig. 12d was approximately $94.4 \mu\text{m}^3$. The material removal volume was therefore $84.1 \mu\text{m}^3$. This result confirms the conclusion in Section 3.3 that the LTS on the ceramic surface can increase the material removal. The volume of material removal on the surface with LTS was approximately 65.6 % larger than that on the polished surface. The large material removal rate may be due to a combination of more defects in the surface layer of the ceramic specimen and the larger tangential load. More defects can lead to grain spalling rather than plastic deformation because crushing occurs via fractures originating at distributed pre-existing flaws where the elastic strain energy density exceeds a critical value [31].

Additionally, the prominent ridges and the small material removal volume of the surface scratch without LTS showed that most material in groove was not eliminated, rather it was extruded on both sides of the groove. This suggests that the scratches were in ductile mode. For the surface with LTS, the ridges and the marks of grain spalling indicated the existence of ductile-brittle mixed mode in the scratches. The ductile-brittle mixed mode is significant for ceramics grinding due to a larger material removal rate in this mode. Grain spalling can also decrease the possibility of crushing to large particles. These phenomena can benefit the surface integrity of the ceramic.

4 Conclusions

A series of scratching tests have been performed on the surfaces with and without LTS to find the differences in material removal behavior between them. The surface hardness, scratching force ratio, scratch groove morphology, and material removal volume were analyzed and compared. The results provide a basis for understanding the material removal mechanism of ceramic grinding although the scratch tests conducted here were quasi-static.

A large temperature gradient was produced on the ceramic surface by LTS. This gradient leads to a decrease in grinding resistance of the ceramic surface. The hardness of the ceramic decreased significantly by 9 % on the surface treated with laser irradiation. The indentation tests indicated that there were obvious microcracks around the indentations on the surface treated with LTS in contrast to few microcracks around the indentations on the surface not treated with LTS. These

microcracks can contribute to grain spalling in the scratch process. However, the reasons for long microcrack generation are not fully understood and are a suitable subject for further research. In scratch tests, the SFR increased dramatically by 16.7 % after the surface was treated with LTS. The groove depth for this LTS-treated surface was approximately 37 % larger than the polished surface. The material removal volume of the scratch on the surface with LTS was larger than without, producing values of 50.8 and $84.1 \mu\text{m}^3$, respectively. The increase was approximately 65.6 %. No microcracks were found on the surfaces with or without LTS while some obvious marks of grain spalling existed on the surface with LTS. These results imply that the material removal mechanism changed from plastic deformation to grain spalling.

These conclusions indicate that laser irradiation on the ceramic surface facilitates material removal due to the existence of the ductile-brittle mixed mode. This is significant for ceramics grinding due to favorable surface integrity and a higher material removal rate. Future research will focus on the damage size induced by LTS and scratching, which can provide greater understanding towards ceramic grinding.

Acknowledgments This research was financially supported by the National Natural Science Foundation of China (Grant no.51475299) and the State Key Laboratory of Mechanical System and Vibration (Grant no. MSVZD201412). The authors are grateful for the editors and reviewers who made constructive comments.

References

1. Horvath M, Kundrak J, Mamalis A, Gyani K (2002) On the precision grinding of advanced ceramics. *Int J Adv Manuf Technol* 20(4):255–258
2. Chen J, Shen J, Huang H, Xu X (2010) Grinding characteristics in high speed grinding of engineering ceramics with brazed diamond wheels. *J Mater Process Technol* 210(6):899–906
3. Agarwal S, Rao PV (2008) Experimental investigation of surface/subsurface damage formation and material removal mechanisms in SiC grinding. *Int J Mach Tools Manuf* 48(6):698–710
4. Kumar M, Melkote S, Lahoti G (2011) Laser-assisted microgrinding of ceramics. *CIRP Ann Manuf Technol* 60(1):367–370
5. Feng P, Liang G, Zhang J (2014) Ultrasonic vibration-assisted scratch characteristics of silicon carbide-reinforced aluminum matrix composites. *Ceram Int* 40(7):10817–10823
6. Samant AN, Dahotre NB (2009) Laser machining of structural ceramics—a review. *J Eur Ceram Soc* 29(6):969–993
7. Desa O, Bahadur S (1999) Material removal and subsurface damage studies in dry and lubricated single-point scratch tests on alumina and silicon nitride. *Wear* 225:1264–1275
8. Zhang B, Zheng X, Tokura H, Yoshikawa M (2003) Grinding induced damage in ceramics. *J Mater Process Technol* 132(1):353–364
9. Zhang X, Chen G, An W, Deng Z, Zhou Z (2014) Experimental investigations of machining characteristics of laser-induced thermal cracking in alumina ceramic wet grinding. *Int J Adv Manuf Technol* 72(9–12):1325–1331

10. Sivakumar R, Jones MI, Hirao K, Kanematsu W (2006) Scratch behavior of SiAlON ceramics. *J Eur Ceram Soc* 26(3):351–359
11. Kanematsu W (2004) Subsurface damage in scratch testing of silicon nitride. *Wear* 256(1):100–107
12. Kun Lee S, Tandon R, Readey MJ, Lawn BR (2000) Scratch damage in zirconia ceramics. *J Am Ceram Soc* 83(6):1428–1432
13. Subhash G, Bandyo R (2005) A new scratch resistance measure for structural ceramics. *J Am Ceram Soc* 88(4):918–925
14. Gu W, Yao Z, Liang X (2011) Material removal of optical glass BK7 during single and double scratch tests. *Wear* 270(3):241–246
15. Azizi A, Mohamadyari M (2015) Modeling and analysis of grinding forces based on the single grit scratch. *Int J Adv Manuf Technol* 78:1223–1231, 1–9
16. Rebro PA, Shin YC, Incropera FP (2004) Design of operating conditions for crackfree laser-assisted machining of mullite. *Int J Mach Tools Manuf* 44(7):677–694
17. Ding H, Shin YC (2013) Improvement of machinability of Waspaloy via laser-assisted machining. *Int J Adv Manuf Technol* 64(1–4):475–486
18. Shen X, Lei S (2011) Experimental study on operating temperature in laser-assisted milling of silicon nitride ceramics. *Int J Adv Manuf Technol* 52(1–4):143–154
19. Peng Y, Liang Z, Wu Y, Guo Y, Wang C (2012) Effect of vibration on surface and tool wear in ultrasonic vibration-assisted scratching of brittle materials. *Int J Adv Manuf Technol* 59(1–4):67–72
20. Zhang X, Chen G, An W, Deng Z, Liu W, Yang C (2014) Experimental study of machining characteristics in laser induced wet grinding silicon nitride. *Mater Manuf Process* 29(11–12):1477–1482
21. Kelly JR, Denry I (2008) Stabilized zirconia as a structural ceramic: an overview. *Dent Mater* 24(3):289–298
22. Backer W, Marshall E, Shaw M (1952) The size effect in metal cutting. *Trans ASME* 74(1):61
23. Ren J, Hua A (2011) The theory of grinding. Publishing House of Electronics Industry
24. Petit F, Ott C, Cambier F (2009) Multiple scratch tests and surface-related fatigue properties of monolithic ceramics and soda lime glass. *J Eur Ceram Soc* 29(8):1299–1307
25. Agarwal S, Rao PV (2013) Predictive modeling of force and power based on a new analytical undeformed chip thickness model in ceramic grinding. *Int J Mach Tools Manuf* 65:68–78
26. Xu HH, Jahanmir S, Ives LK (1996) Material removal and damage formation mechanisms in grinding silicon nitride. *J Mater Res* 11(07):1717–1724
27. Ben LCGHW, Renke GDTXK, Dongjiang W (2010) Experimental study of single-tip scratching on potassium dihydrogen phosphate single crystal [J]. *J Mech Eng* 13:027
28. Marinescu ID, Hitchiner MP, Uhlmann E, Rowe WB, Inasaki I (2006) Handbook of machining with grinding wheels. CRC Press
29. Liang Z, Wang X, Wu Y, Xie L, Liu Z, Zhao W (2012) An investigation on wear mechanism of resin-bonded diamond wheel in elliptical ultrasonic assisted grinding (EUAG) of monocrystal sapphire. *J Mater Process Technol* 212(4):868–876
30. Zhang W, Subhash G (2001) An elastic–plastic–cracking model for finite element analysis of indentation cracking in brittle materials. *Int J Solids Struct* 38(34):5893–5913
31. Larchuk T, Conway J, Kirchner H (1985) Crushing as a mechanism of material removal during abrasive machining. *J Am Ceram Soc* 68(4):209–215